Distributed Sequential Coalition Formation Algorithm for Spectrum Allocation in Underlay Cognitive Radio Networks

Wei Liang, *Member, IEEE*, Kai Di Wang, *Student Member, IEEE*, Jia Shi, *Member, IEEE*, Lixin Li, *Member, IEEE* and George K. Karagiannidis, *Fellow, IEEE*

***Abstract*— In this paper, we study the resource allocation problem, including the joint consideration of user grouping and power allocation, of an underlay cognitive radio (CR) network employing non-orthogonal multiple access (NOMA), which is referred to as NOMA-CR network. Based on the non-transferable utility coalition formation game theory, the so-called distributed sequential coalition formation (DSCF) algorithm is leveraged to solve the user grouping problem, where multiple cognitive users within a group can access the primary user's spectrum band, while satisfying a minimum rate requirement of the primary user. Simulation results show that a near-optimal performance can be achieved by implementing the proposed DSCF as well as the optimal power allocation algorithms. Furthermore, the results validate that NOMA-CR can significantly outperform the traditional orthogonal multiple access CR, in terms of throughput. Finally, it is shown that by applying a novel adaptive trellis turbo coded modulation technique to the underlay NOMA-CR network, a significant throughput gain can be achieved.**

***Index Terms*— Cognitive radio network, NOMA, User grouping, Coalition formation game, merge-and-split game.**

I. Introduction

In wireless communications, cognitive radio (CR) constitutes a design paradigm for a network or a wireless node, which could change its transmission mode efficiently, such that the unlicensed users/cognitive users (CUs) could communicate, while the licensed users/primary users (PUs) are silent, in order to avoid the interference. In Haykin's pioneering paper [1], it was stated that a CR constitutes a highly reliable communications device ensuring that the radio spectrum can be efficient exploited. Goldsmith *et al.* in [2] proposed three main paradigms for spectrum access in CR networks: *underlay*, *overlay* and *interwave* networks. In the underlay CR network, the CUs can transmit simultaneously with PUs by using the same frequency band, under the constraint that the interference created by the CUs on the PUs does not degrade the PU's communication quality. In this scheme, the CUs are not required to perform spectrum sensing. However, the interference caused by the CUs' must not exceed a tolerable threshold [3].

Non-orthogonal multiple access (NOMA) was emerged as a promising multiple access (MA) technique to improve the capacity of the future mobile networks [4]–[7]. Additionally, the concept of NOMA has been applied in several research areas, as in cooperative communications [8], [9], multiple-input multiple-output (MIMO) systems [10], high-rate visible light communication (VLC) networks [11], simultaneous wireless information and power transfer (SWIPT) [12], cognitive radio networks [13] as well as in the physical layer security [14]. The key idea of NOMA is to explore the power domain for MA. More specifically, in the downlink NOMA, a base station (BS) can serve multiple users within the same time/frequency channel via different power allocations, where to the users with poor channel conditions is allocated more transmission power. Therefore, these users are capable of decoding their own messages by treating the other users' information as noise. On the other hand, the users with lower allocated power employ successive interference cancellation (SIC) to decode their own messages, by first removing the other users' information from their observations. Furthermore, by discussing the aforementioned two concepts, NOMA can be also used in underlay CR networks in order to improve the system's spectral efficiency. In [15], a stochastic geometry model was proposed for a large-scale CR network, while the application of NOMA to cooperative spectrum sharing CR networks was investigated in [16]. Specifically, the authors in [15]–[17] used stochastic geometry to characterize the outage performance of the combined concept of NOMA and CR. Additionally, an open issue is to efficiently group the users in the considered underlay CR-NOMA networks.

As a highly appealing mathematical tool, game theory can resolve various problems in cooperation or competition scenarios. Specifically, cooperative game theory has been widely used in wireless communication, where especially the coalition formation game [18]–[24] was proposed to describe user coalitions among the users. Specifically, in [18] a fair cooperation strategy among distributed single antenna transmitters was proposed, which allows users to be self-organized into structured coalitions, aiming to maximize the considered utilities. The authors in [19] have developed a new cooperation pattern, which allows multiple CU pairs to access the same

Corresponding author: Jia Shi (jiashi@xidian.edu.cn).

The work was supported by the Fundamental Research Funds for the Central Universities Grant3102018QD096.

W. Liang and L.X. Li are with school of Electronic Information Collage, Northwestern Polytechnical University, China. Email: {liangwei, lilixin}@nwpu.edu.cn.

K. D. Wang is with school of Electrical and Electronic Engineering, University of Manchester, UK. Email:kaidi.wang@postgrad.manchester.ac.uk.

J. Shi is with State Key Lab. of Integrated Services Networks, Xidian University, China. Email:jiashi@xidian.edu.cn.

G. K. Karagiannidis is with the Wireless Communication System Group, Electrical and Computer Engineering Department, Aristotle University of Thessaloniki, Greece. Email: geokarag@auth.gr.

This article has been accepted for publication in a future issue of this journal, but has not been fully edited. Content may change prior to final publication. Citation information: DOI 10.1109/ACCESS.2019.2910720, IEEE Access

spectrum of the PU. However, by using a fixed order these CUs are allowed to access the spectrum sequentially, in order to maximize their own benefits. Furthermore in [20], each CU is modeled as a player to maximize its individual utility, that captures the expected throughput and energy efficiency. Additionally, the distributed collaboration strategies for CU grouping in a cognitive network was proposed in [21], where each CU decides to form or break a coalition, aiming to maximize the individual utility. Moreover, in this paper, the management of spectrum resources, based on a coalition game with transferable utility, has been also investigated. Different to this work, the authors in [22] have studied the resource allocation problem in Device to Device (D2D) cellular networks through game theory. Specifically, each user can only participate in one sub-game at a time, but can change its behavior to leave the current sub-game and join into another one in order to improve their own utilities.

Scanning the open literature and to the best of the authors's knowledge, there is no any research work which uses the coalition formation game theory to solve the resource allocation problem in NOMA aided underlay CR networks. In this paper we present for first time an underlay CR network model with NOMA, in which the joint problem of user grouping and power allocation is investigated. The key contributions of this paper can be summarized as follow:

- We present an underlay CR network with NOMA, referred to as a CR-NOMA, where the CUs are formed user groups/coliations and the best one is selected to access the PU's spectrum band, subject to the PU's Quality of Service (QoS). Furthermore, we formulate the resource allocation problem, which can be decoupling into two sub-problems: user grouping and power allocation. The original optimization problem is a mixed integer non-linear programming and can be tackled by subsequently solving the two decoupled sub-problems.
- In order to solve the user grouping problem, we propose a distributed sequential coaction formation (DSCF) algorithm, which is based on the coalition formation game theory with non-transferable utility (NTU). In this algorithm, we consider the 'merge-and-split' rule to decide whether a CU is split from or merged into a current group, based on its own interest and aiming to maximize the system's utility. Moreover, it is shown that the DSCF algorithm is stable and requires significantly lower complexity than the centralized algorithm, which is considered as benchmark. Furthermore, an optimal power allocation algorithm is proposed, based on the stable user grouping partitions. In particular, the original non-convex power allocation problem is converted into a convex one by employing first order Taylor approximation as well as other manipulations, and it is proved that the solution converges to a Karush-Kuhn-Tucker (KKT) point with a small number of iterations.
- We investigate the practical designs of the bandwidth-efficient adaptive trellis turbo coded modulation (ATTCM) in the considered CR-NOMA network, in order to further improve the network's throughput. The transmission rate/throughput of the system is adapted according to the instantaneous channel conditions. A higher-throughput but vulnerable TTCM scheme is employed when the channel conditions are good, while a lower-throughput but robust TTCM scheme or no transmission is used, when the channel conditions are poor.
- Finally, we perform simulations for the underlay CR-NOMA network by employing the proposed DSCF algorithm and the optimal power allocation algorithm. Numerical results show that the system throughput of the CR-NOMA significantly outperforms the traditional CR-OMA, which illustrates the importance of NOMA. Furthermore, we demonstrate that the proposed DSCF algorithm can always obtain stable CU groups/coalitions and can achieve a near-optimal solution. Finally, we prove the optimality of the proposed power allocation algorithm.

The rest of the paper is organized as follows. The system model and problem formulation are outlined in Section II. The proposed user grouping algorithm is given in Section III. Then, the power allocation algorithms are discussed in Section IV. Additionally, a practical adaptive coded modulation scheme is described in Section VI. The simulation results are provided in Section V. Finally, the conclusions are presented in Section VII.

II. System Model and Problem Formulation

A. System Model

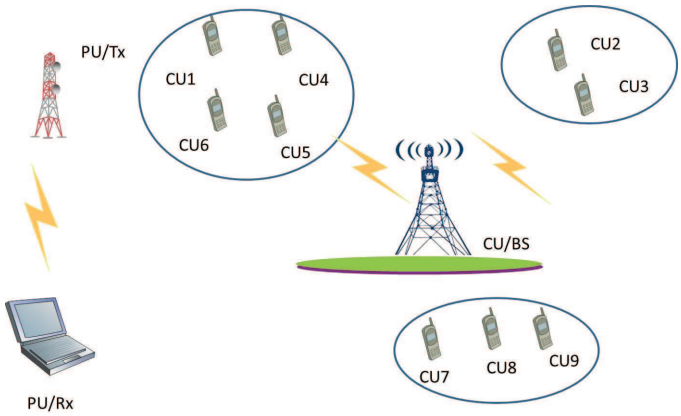

Fig. 1. The system model of an underlay NOMA-CR network conceived.

In this paper, an underlay CR network is considered in Fig. 1, which consists of one pair of PU transmitter (Pt) and PU receiver (Pr) [1] and a cluster of CUs [2]. As depicted in Fig. 1, if the downlink NOMA-CR network is considered, the Pt transmits information to the Pr, which is interfered by as well as creates interference to the CU. In contrast to the existing literature, multiple CUs within the same group are allowed to access the PU's spectrum band simultaneously, as long as the interference to PU is tolerable. By performing user grouping, the CUs are formed into different groups, and one CU group

[1]A Pt-Pr pair constitutes the PU's transceiver. PU acting as source node is referred to as Pt, while PU acting as destination node is denoted by Pr.

[2]In the CUs' transmission, a cognitive base station (C-BS) is denoted as the CU's transmitter, and the multiple CUs' receivers are referred by Ct.

This article has been accepted for publication in a future issue of this journal, but has not been fully edited. Content may change prior to final publication. Citation information: DOI 10.1109/ACCESS.2019.2910720, IEEE Access

is selected to access the PU's spectrum simultaneously. This is to avoid the overcrowded CUs' groups be accessed to the same PU's spectrum. To achieve interference-free among user groups, different user groups will be allocated orthogonal frequency bands to perform orthogonal multiple access (OMA), in order to guarantee certain QoS requirements. With the aid of NOMA, CUs within the same group are capable of accessing the same spectrum simultaneously.

The mathematical model of the NOMA-CR network under investigation is described below. A cognitive base station (C-BS) is located at the origin of a disc $\mathcal{D}_i$ with radius one. The distance between the Pt (Ct) and the Pr (Cr) is denoted by $d_{Pt,Pr}$ ($d_{Ct,Cr}$), while the interference link distance between a Pt (Ct) and a Cr (Pr) is denoted by $d_{Pt,Cr}$ ($d_{Ct,Pr}$). The K CUs are randomly deployed in a disc $\mathcal{D}_c$ and thus holds $0 < d_{Ct,Cr_k} < 1$. The Pt and Pr are assumed to locate on the opposite sides of square $\mathcal{D}_o$ with the side length being two, which is outside $\mathcal{D}_o$. Hence, the Pt-Pr distance is $d_{Pt,Pr} = 4.0$, and the interference link distance between the Pt and a Cr belongs the range of $1 < d_{Pt,Cr_k} < 3$. Note that in this underlay CR paradigm, the interference threshold for PU's transmission is pre-determined as I_{th}. For clarity, the other key notations and parameters are summarized in Table I.

Notation	Definition
K	Number of CUs
$\mathcal{K}$	Set of CU indexes
L	Number of user coalitions
$\mathcal{L}$	Set of CU group indexes
P_p	PU's transmit power
P_c or P_s	CU's transmit power
R_{req}^{PU}	Minimum rate requirement of PU
$\mathcal{A}$	Power allocation matrix
a	Power allocation factor
$\mathcal{M}$	CU grouping matrix
$\mathcal{S}_l$	Set of CU indexes in group l

TABLE I
MAIN NOTATIONS OF THE CR-NOMA SYSTEM MODEL.

1) Achievable Rate of the PU: The signal received by the Pr can be written as:

$$Y_{Pt,Pr} = \sqrt{P_p} h_{Pt,Pr} X_p + \sqrt{P_c} h_{Ct,Pr} X_c + n_p \ , \quad (1)$$

where $h_{Pt,Pr}$ denotes the channel gain between the Pt and Pr, and $h_{Ct,Pr}$ represents the channel gain between the Ct and Pr. In Eq. (1), X_p and X_c are the information for PU and CU, respectively. Furthermore, n_p is the Gaussian noise term, which follows Gaussian distribution with zero mean and variance $N_0/2$ per dimension. Based on Eq. (1), if one CU group accesses the PU's spectrum, the achievable rate of the PU can be given by

$$R_{PU}(\mathcal{S}_l) = \log_2 \left(1 + \frac{|h_{Pt,Pr}|^2 P_p}{I_{Ct,Pr} + \sigma^2} \right) . \quad (2)$$

In Eq. (2), $I_{Ct,Pr}$ denotes the interference of the PU imposed by the CU, which can be expressed as

$$I_{Ct,Pr} = |h_{Ct,Pr}|^2 P_c \ . \quad (3)$$

If there is no CU accessing the PU's spectrum, the achievable rate of the PU becomes

$$R_{PU}(\emptyset) = \log_2 \left(1 + \frac{|h_{Pt,Pr}|^2 P_p}{\sigma^2} \right) . \quad (4)$$

If the PU's minimum rate requirement is $R_{req}^{PU} = R_{PU}(\emptyset)$, then, when a CU group is allowed to access the PU's spectrum, the achievable rate of the PU should be greater than its minimum rate requirement:

$$R_{PU}(\mathcal{S}_l) \geq \eta R_{req}^{PU} \ . \quad (5)$$

In Eq. (5), $\eta < 1$ is a positive scale factor, defined by the PU and can be adjusted according to different demands [19]. This factor aims to achieve a relatively small target data rate of the PU when the interference can be tolerated. In the underlay NOMA-CR network, the transmit power of the C-BS should be restricted according to the performance of the primary transmission. Then, by using Eq. (2), Eq. (4) and Eq. (5), the P_c can be derived as:

$$P_c \leq \frac{1}{|h_{Ct,Pr}|^2} \left(\frac{P_p |h_{Pt,Pr}|^2 - \sigma^2}{2^{\eta R_{req}^{PU}} - 1} \right) . \quad (6)$$

Note that, Eq. (6) denotes the maximum permissible interference power at the Pr, which ensures the undesired CU's interference at the Pr can be controlled, by imposing a limit on the maximum transmitting power of the C-BS.

2) Achievable Rate of CUs: In the underlay scheme, the C-BS utilizes the PU's spectrum to send a combined information to all CUs, and the received signal at CU_k is given by

$$Y_k^{CU} = h_{Ct,Cr_k} \sum_{k=1}^{K} \sqrt{a_k P_c} X_c + n_c \ , \quad (7)$$

where a_k denotes the power allocation coefficient for CU_k, and h_{Ct,Cr_k} is the channel gain between the C-BS and Cr_k. n_c is the Gaussian noise term, which follows Gaussian distribution with a zero mean and a noise variance of $N_0/2$ per dimension and X_c is the information of the CU_k. By using Eq. (6), the transmit power P_c at the C-BS is constrained as [25]:

$$P_c = \min \left[\frac{1}{|h_{Ct,Pr}|^2} \left(\frac{\gamma_p |h_{Pt,Pr}|^2}{2^{\eta R_{req}^{PU}} - 1} \right), P_s \right] , \quad (8)$$

where P_s is the maximum transmission power at the C-BS.

Additionally, we assume that the total power coefficients of the CUs in each group is one, i.e. $\sum^{F(F<K)} \alpha_k = 1$. Without loss of generality, we assume that, the channel gains of CUs follow the order $|h_{Ct,Cr_1}|^2 \leq |h_{Ct,Cr_2}| \leq \cdots \leq |h_{Ct,Cr_K}|^2$. When NOMA is used, the power allocation coefficients should satisfy $a_1 \geq a_2 \geq \cdots \geq a_K$. In the line of [8], successive interference cancellation (SIC) technique is carried out at the receiver of the CUs. The achievable rate of the CU depends on the users within the same group. Suppose that, CU_1, CU_2 and CU_3 are in the same group $\mathcal{S}_l$, and their channel gains follow: $|h_1|^2 \leq |h_2|^2 \leq |h_3|^2$. In this case, CU_2 can decode the message from CU_1 and treat CU_3's message as interference. Particularly, CU_3 first decodes the messages of both CU_1 and CU_2, and then successively subtracts these messages to obtain its own message. Additionally, since CU_1 has the worst channel condition in $\mathcal{S}_l$, it will treat all other users' message as its noise. Then, according to the principle of NOMA scheme, the achievable rate of CU_k in the group is given by

$$R_k^{CU} = \log_2 \left(1 + \frac{|h_{Ct,Cr_k}|^2 P_c a_k}{|h_{Ct,Cr_k}|^2 P_c \sum_j^F \alpha_j P_c + P_p |h_{Pt,Cr_k}|^2 + \sigma^2} \right) , \quad (9$$

This article has been accepted for publication in a future issue of this journal, but has not been fully edited. Content may change prior to final publication. Citation information: DOI 10.1109/ACCESS.2019.2910720, IEEE Access

where $P_P|h_{Pt,Cr_k}|^2$ denotes the interference from the Pt to the CUs' receiver. Note that, the achievable rate of CU_K can be computed as

$$R_K^{CU} = \log_2\left(1+\frac{|h_{Ct,Cr_K}|^2 P_c}{P_p|h_{Pt,Cr_k}|+\sigma^2}\right) . \quad (10)$$

Therefore, the sum rate of CUs in one group is given by

$$R_l^{CU}(\mathcal{S}_l) = \sum_k^{|\mathcal{S}_l|} R_k^{CU} . \quad (11)$$

To ensure fairness, we introduce the weighted sum rate of the CUs in group $\mathcal{S}_l$, given by

$$\tilde{R}_l^{CU}(\mathcal{S}_l) = \sum_k^{|\mathcal{S}_l|} w_{k,l} R_k^{CU} , \quad (12)$$

where $w_{l,k}$ is the weight factor and defined as $w_{l,k} = \frac{|h_{Ct,Cr_k}|}{\max\{|h_{Ct,Cr_k}|\}}$. By using this weight factor among all CUs, the utility of the CU with the best channel condition can be scaled, and has less impact on the CU who has the worst channel condition within the same CU group. In that case, it gives us more flexibility to configure our system design.

B. Problem Formulation

In the network, under consideration the resource allocation, including user grouping and power allocation aims to maximize the network throughput utility. The corresponding optimization problem can be expressed as

$$\max_{\mathbf{A},\mathbf{M}} \sum_{l\in\mathcal{L}}\sum_{k\in\mathcal{K}} m_{k,l} U(\mathcal{S}_l) , \quad (13)$$

$$\begin{aligned} s.t.\quad & (a)\ \sum_{k\in\mathcal{S}_l} a_{k,l} = 1 \ , \forall l \in \mathcal{L} \\ & (b)\ 1 > a_{k,l} > 0 \ , \forall k \in \mathcal{K}, \forall l \in \mathcal{L} \\ & (c)\ \sum_{l\in\mathcal{L}} m_{k,l} = 1 \ , \ \forall k \in \mathcal{K}, \\ & (d)\ m_{k,l} \in \{0,1\} \ , \forall k \in \mathcal{K}, \forall l \in \mathcal{L} . \end{aligned}$$

In Eq. (13), $U(\mathcal{S}_l)$ is the utility reflected by summing up the weighted sum rate of the CUs given by Eq. (12) and the achievable rate of the PU described by Eq. (2). Define that, $\mathbf{M}$ is a $(K \times L)$-element CU grouping matrix. When CU_k is in group $\mathcal{S}_l$, the corresponding entry is given by $m_{k,l} = 1$, otherwise $m_{k,l} = 0$. Further, $\mathbf{A}$ is a (K)-element power allocation vector with elements $a_{k,l}$ for group $\mathcal{S}_l$. In problem (13), $\mathcal{S}_l$ is the set collecting the indexes of the CUs in group l, and it can be mapped from the user grouping matrix $\mathbf{M}$. Constraint (a) ensures the sum of the power allocation factor in each coalition is one. Condition (b) implies the range of the power allocation constraint of each CU. The condition (c) indicates that each CU will only be joined into one group. Note that, the total transmit power P_p for Pt is a parameter predefined according to system requirement, and the total transmit power P_c for C-BS follows the constraint of Eq. (8).

Specifically, the optimization problem in Eq. (13) is known as a mixed integer non-linear programming (MINLP) and it is NP-hard. Additionally, this problem can be decoupled with respect to two entries, which are the optimal power allocation matrix $\mathbf{P}$ and the optimal coalition matrix $\mathbf{M}$. Next, we solve this optimization problem in two steps. Specifically, with a fixed power allocation, the user grouping problem is solved with the aid of game theory, where in particular, the cooperative game model is applied. Note that, the final user partitions of the CUs were satisfied the predefined QoS requirements of the PU. Then, based on the user grouping power allocation for the CUs is implemented.

III. Coalition Formation Game Aided User Grouping

In this section, we resort non-transferable utility (NTU) coalition formation game model to solve the user grouping problem in the underlay CR-NOMA network. Specifically, a so-called Distributed Sequential Coalition Formation algorithm is proposed, in which a stable coalition structure for CU grouping can be obtained via a distributed manner.

A. Coalition Formation Game

According to the game theory terminology, we refer to the CUs as players, and the coalition value function is denoted by U. Then the user group can be modeled as an $(\mathcal{N}, U)$ coalition formation game in characteristic form, where $\mathcal{N}$ represents the partition of this game model. The arbitrary groups/coalitions [3] are defined as $\mathcal{S}_l \in \{\mathcal{S}_1, \cdots, \mathcal{S}_L\}$, in which L is the number of user groups. Therefore, the coalition value function can be expressed as

$$\begin{aligned} U(\mathcal{S}_l) &= \varphi(\mathcal{S}_l) \\ &= (\varphi_1(\mathcal{S}_l), \cdots, \varphi_{|\mathcal{S}_l|}(\mathcal{S}_l)), \ \forall l \in \{1, \cdots, L\} \end{aligned} \quad (14)$$

where $\varphi_j(\mathcal{S}_l)$ is the individual pay-off of each player in coalition $\mathcal{S}_l$. Then, it is given by

$$\varphi_j(\mathcal{S}_l) = \begin{cases} R_j^{CU}(\mathcal{S}_l), & \text{if Eq. (5), (6) are met ;} \\ 0, & \text{Otherwise .} \end{cases} \quad (15)$$

To further study the coalition formation game model, we introduce the following definitions.

Definition 1: A collection of coalitions, namely $\mathcal{C}$, can be defined as $\mathcal{C} = \{\mathcal{S}_1, \mathcal{S}_2, \cdots, \mathcal{S}_L\}$, where $\mathcal{S}_l \subseteq \mathcal{N}$. Specifically, a collection defines an arbitrary group of disjoint coalitions. The collection $\mathcal{C}$ is defined as a partition of $\mathcal{N}$, while this collection spans all players in $\mathcal{N}$.

Definition 2: We have two collections, namely $\mathcal{C} = \{\mathcal{S}_1, \mathcal{S}_2, \cdots, \mathcal{S}_L\}$ and $\mathcal{C}' = \{\mathcal{S}_1', \mathcal{S}_2', \cdots, \mathcal{S}_L'\}$, which are the two different partitions of the same subset $\mathcal{B} \subseteq \mathcal{N}$. Then a preference operation or comparison relation $\triangleright$ is defined for comparing these two collections, i.e. $\mathcal{C}$ and $\mathcal{C}'$. Thus, $\mathcal{C} \triangleright \mathcal{C}'$ illustrates the way $\mathcal{C}$ partitions $\mathcal{B}$ is preferred to the way $\mathcal{C}'$ partitions $\mathcal{B}$.

Based on the coalition formation game model, the objective of each player is to obtain a higher individual payoff by splitting or merging a new coalition, if joining into this new

[3]'group' can be referred as 'coalition' in the coalition formation game.

This article has been accepted for publication in a future issue of this journal, but has not been fully edited. Content may change prior to final publication. Citation information: DOI 10.1109/ACCESS.2019.2910720, IEEE Access

coalition can bring a higher individual payoff compared with the previous one. Therefore, the definitions of "merge" and "split" are given as follows.

Definition 3: Merge Rule: Any set of coalitions $\{\mathcal{S}_1, \cdots, \mathcal{S}_L\}$ may be merged whenever the merged behavior is preferred by the players; i.e.where $\{\cup_{l=1}^{L}\mathcal{S}_l\} \triangleright \{\mathcal{S}_1, \cdots, \mathcal{S}_\mathcal{L}\}$, therefore $\{\mathcal{S}_1, \cdots, \mathcal{S}_\mathcal{L}\} \rightarrow \{\cup_{l=1}^{L}\mathcal{S}_l\}$.

Definition 4: Split Rule: Any coalition $\cup_{l=1}^{L}\mathcal{S}_l$ may be split whenever a split form is preferred by the players; i.e. where $\{\mathcal{S}_1, \cdots, \mathcal{S}_L\} \triangleright \{\cup_{l=1}^{L}\mathcal{S}_l\}$, thus, $\{\cup_{l=1}^{L}\mathcal{S}_l\} \rightarrow \{\mathcal{S}_1, \cdots, \mathcal{S}_\mathcal{L}\}$.

By considering the *Definition 3* and *Definition 4*, a small coalition could split from a large coalitions if the splitting yields a more preferred collection, based on the selected order. On the contrary, multiple coalitions can merge into a large coalition if merging yields a better collection. By using merge-and-split rules, the coalitions will split (or merge) only if at least one CU is capable of improving its individual pay-off, while not degrading the total CUs' payoff of this coalition. In this paper, the objective of user grouping is to find the optimal coalition structure, aiming to maximize the system's utility. For this sake, next we propose the Distributed Sequential Coalition Formation (DSCF) algorithm.

B. Distributed Sequential Coalition Formation algorithm

As described in Section II-B, the combination of user grouping and power allocation problem has been presented in Eq. (13), which can be decoupled to first solve the user grouping problem upon given a fixed power allocation. The corresponding optimization problem can be written as

$$\max_{\mathbf{M}} \left\{ \sum_{l\in\mathcal{L}} \sum_{k}^{K} m_{k,l} U(\mathcal{S}) \mid \mathbf{A}^* \right\}, \tag{16}$$

$$s.t. \quad (a) \ \sum_{l\in\mathcal{L}} m_{k,l} = 1 \ , \forall k \in \mathcal{K} \ ,$$
$$(b) \ m_{k,l} \in \{0,1\} \ , \forall k \in \mathcal{K}, \forall l \in \mathcal{L} \ .$$

Nevertheless, the constraint in Eq. (16)(b) contains the binary variables $\{m_{k,l}\}$, which makes the user grouping problem very difficult to tackle. As it is well known, the widely-used method for solving this problem requiring the relaxation of variables $\{m_{k,l}\}$, which may lead to poor suboptimal solutions. In contrast, cooperative game theoretic, specifically the coalition formation game, can be employed to efficiently solve this problem.

With the aid of the basic definitions given in Section III-A, the key idea of the proposed distributed sequential coalition formation (DSCF) algorithm is to utilize the merge and split rules to find the optimal coalitions, i.e. the best user grouping, in the context of the CR-NOMA system. Specifically, the players (CUs) can merge into or split out any coalitions based on their own benefits. Refer to Algorithm 1, the details of the DSCF algorithm are elaborated as follows.

At the initialization phase of Algorithm 1, the PU announces his demand to all the CUs according to Eq. (5). In steps (1) and (2), all the CUs are staying in the non-cooperative states, which result in multiple independent coalitions. In particular, the CUs who have the worst channel conditions will construct their fixed independent coalitions. This is because these users may need more transmit power due to NOMA, albeit they are not capable of merging into other groups according to the merger rule. Furthermore, let us set the channel gain threshold, namely h_t, to identify the CUs with poor channel conditions. In this case, the CUs with channel gains below h_t are formed as the independent coalitions. In other words, the CUs whose position are close to the worst user will be treated as the fixed coalitions. Let the number of the fixed coalitions to be Mx.

During step 2 of Algorithm 1, the N active CUs, which have not joined into the fixed coalitions, are sorted in a descending order based on their channel conditions, determined by the order of ρ. Accordingly, the CU with the highest channel condition (i.e. with the highest rank) makes a move firstly, while the others are kept silence. We assume that, during each step an active CU only cares about its own avenue, and chooses a coalition, which results in the highest individual pay-off, and to join into. Note that, the coalitions are formed iteratively for each CU, such as CU_n $\forall n \in N$. At each iteration, we first set the pay-off of active CU_n to zero, which means it originally keeps quiet. Then, CU_n calculates its pay-off in a candidate coalition based on Eq. (9), and after comparision it with its previous pay-off. If a new partition is formed, the corresponding pay-off will update. The N active CUs jump from one coalition to another, until the stable partition are obtained. Importantly, the process of "merge" and "split" converges to a final partition which is independent of the selected order or the initial condition of the network. Moreover, the coalition forming process will be terminated if the maximum number of iterations itr_{max} is exceed in order to keep the implementation complexity in an acceptable level. In the final stage, no CU has the willing to deviate from its current coalition and to form a new coalition based on the merge and split rule. Therefore, the best coalition, i.e. CU group, which gives the highest sum rate, is selected to access the PU's spectrum, subject to meeting the PU's minimum rate requirement.

To the following example we explain the algorithm in more details. Assume that, the underlay CR network has K CUs, denoting as $K = \{1, 2, 3, 4, 5, 6, 7\}$. Without loss of generality, we have $|h_1|^2 < |h_2|^2 < |h_3|^2 < |h_t|^2 < |h_4|^2 < |h_5|^2 < |h_6|^2 < |h_7|^2$. Furthermore, there are three fixed coalitions, which are $\mathcal{S}_1 = \{1\}$, $\mathcal{S}_2 = \{2\}$ and $\mathcal{S}_3 = \{3\}$. For the other four CUs we can get the order $\rho = \{7, 6, 5, 4\}$, which corredponds to the channel conditions from the highest to the lowest. For initialization, we keep these four CUs silent. During the first iteration, CU_7 makes the first choice (i.e. $\rho(1) = 7$). Assume that CU_7 prefers coalition $\mathcal{S}_1$ over $\mathcal{S}_2$ and $\mathcal{S}_3$, then CU_7 chooses $\mathcal{S}_1$ to join in. After that, CU_6 ranks second from the order ρ, and start to make its choice. Assume that, $\mathcal{U}_6(\mathcal{S}_1) \triangleright \mathcal{U}_6(\mathcal{S}_3) \triangleright \mathcal{U}_6(\mathcal{S}_2)$, CU_6 chooses to join coalition $\mathcal{S}_2$. For CU_5 which is ranking third in ρ, assume that $\mathcal{U}_5(\mathcal{S}_1) \triangleright \mathcal{U}_5(\mathcal{S}_2) \triangleright \mathcal{U}_5(\mathcal{S}_3)$. Then CU_5 joins in coalition $\mathcal{S}_3$. Finally, the last CU of the order ρ makes a decision. As known, the own pay-off of CU_4 in $\mathcal{S}_2$ and $\mathcal{S}_3$ is lower than it in $\mathcal{S}_1$. Hence, CU_4 chooses to stay in coalition $\mathcal{S}_1$. Therefore, the final partition is $\Pi^{(7)} = \{\{1, 4, 7\}_{\mathcal{S}_1}, \{2, 6\}_{\mathcal{S}_2}, \{3, 5\}_{\mathcal{S}_3}\}$.

This article has been accepted for publication in a future issue of this journal, but has not been fully edited. Content may change prior to final publication. Citation information: DOI 10.1109/ACCESS.2019.2910720, IEEE Access

Algorithm 1: Distributed Sequential Coalition Formation

Step 1: Initialization

1) The PU announces η to K CUs.
2) Set the initial partition state as $\mathcal{C}_{ini} = \{\mathcal{S}_1, \cdots, \mathcal{S}_L\}$, where $L = K$.
3) Identify M_x CUs (with worst channel conditions while satisfying $h_{ct_k,cr_k} \leq h_t$) of each forming a fixed coalition, where h_t is the pre-determined channel gain threshold.
4) Set iteration index $itr = 0$, and maximum itr_{max} allowed;

Step 2: Play the game

1) Sorting the N ($N = K - M_x$) active/unidentified CUs according to their channel conditions.
2) These N CUs make coalition decisions one by one according to their order list ρ.
3) The nth CU merges into a coalition if satisfying the *Merge Rule* in Definition 3.
   - If $\mathcal{U}_n(\emptyset) \triangleright \mathcal{U}_n(\mathcal{S}_l)$, then construct tentative coalitions and do the SIA order as described in Algorithm 2.
4) The nth CU splits from the current coalition if meeting the *Split Rule* in Definition 4.
   - If $\mathcal{U}_n(\mathcal{S}_l) \triangleright \mathcal{U}_n(\mathcal{S}_{l+1})$, then form a new coalition.

Step 3: Update index $itr = itr + 1$ *and Repeat Step 2*

Until 1) the partition converges to a final stable partition; or 2) $itr \geq itr_{max}$.

Step 4: Establish cooperation with PU

The PU selects the coalition which has the highest sum rate while its minimum rate requirement is met.

C. Stability Analysis

In the proposed DSCF algorithm, it can be derived a constructed partition consisting of multiple disjoint coalitions. For proving the final partition is stable. Let us make the following definition, i.e. Nash-stable [26].

Definition 5: A partition structure $\mathcal{C} = \{\mathcal{S}_1, \mathcal{S}_2, \ldots, \mathcal{S}_L\}$ is Nash-stable if $\forall R_l \in \Re$, $\mathcal{C}' \triangleright \mathcal{C}$, where $\mathcal{C}' = \{\mathcal{S}_1, \mathcal{S}_2, \ldots, \mathcal{S}_l - \mathcal{R}_l, \ldots, \mathcal{S}_q \bigcup \mathcal{R}_l, \ldots, \mathcal{S}_L\}$, and $\mathcal{S}_q \neq \mathcal{S}_l$.

According to Definition 5, a partition structure is stable if there is no player k, where $k \in \mathcal{K}$, in the game has an incentive to split its current coalition $\mathcal{S}_l$, and merges into other coalitions $\mathcal{S}_j$. Hence, a stable partition implies that there are no players in their current partitions would be beneficial by joining into the other coalitions. Meanwhile, the actions of the players, (merge or split), would not reduce the other players' corresponding utilities within the same coalition, such as:

$$\begin{aligned} &\varphi_l(\mathcal{S}_l) > \varphi_l(\mathcal{S}_l \cup \mathcal{R}_l) \\ s.t.\ \ &\varphi_l(\mathcal{S}_l - \mathcal{R}_q) < \varphi_l(\mathcal{S}_l)\ , \forall \mathcal{R}_l \in \mathcal{L}\ . \end{aligned} \tag{17}$$

According to the above definition, we may derive the following proposition.

Proposition 1: The DSCF algorithm can converge to a *Nash-stable* coalition structure $\mathcal{C}$.

Proof: At the beginning of our proposed algorithm, the payoff for each player is assumed to zero. Thus, there are no players who refuse to join any fixed coalition, since a better payoff of each player can be obtained by merging them into the coalitions. As a result, the active players in the system would like to have a action whether to join into or merge from the coalition.If a player prefers to another coalition. Such as, active player N will be moved from $\mathcal{S}_i$ to $\mathcal{S}_l$ via an iterative merge-and-split operation as shown in Algorithm 1. This implies that the current obtained collections $\mathcal{C}$ is not stable. Further, the iterative merge-and-split operation terminates until all the players satisfy with their current coalitions. Therefore, in a Nash-stable coalition structure, no one has an incentive to leave its current coalition.

D. Complexity Analysis

In this section, We analyze the complexity of the proposed DSCF algorithm. The number of operations/cycle to used to reflect the complexity of the proposed algorithm. Apparently, the complexity of the DSCF algorithm is closely related to the number of the merge-and-split operations [27].

As described in Algorithm 1, we have M_x fixed coalitions according to the channel condition threshold h_t. Then the number of active CUs who are intending to join into the fixed coalitions is $(K - M_x)$. Additionally, the fixed coalitions with the steady CUs are subject to the merge operations. Those steady CUs are not able to ally with each other. Hence the total number of merge attempts is M_x. Additionally, the split rule is a complex process, since all the possible partitions of the collections formed by the active CUs. However, the split operations are only applied to the fixed coalitions. That is because the steady CUs will not split from their coalitions, if it is stable. Therefore, the worst case is that each active CU cannot join into the other coalitions or the user's structure is singleton. In that case, each active CU tries to merge into $(K - M_x - 1)$ coalitions. Hence, there are M_x times of calculations for each active CU.

Additionally, the computational complexity of DSCF algorithm can be expressed as: $\mathcal{O}(QKM_x - QM_x^2)$, where assuming that the number of cycle time (or number of iterations) is Q.. Therefore, the merge complexity linearly varies with the number of the steady CUs, and the split complexity is related to the number of the selected active CUs.

IV. Power Allocation Algorithms

In this section, we will introduce two power allocation algorithms, which include the conventional power allocation

and the proposed optimal power allocation algorithms.

A. Problem Formulation

After operating the DSCF algorithm as described in Section III-B, we obtain a stable coalition structure. After decoupling problem (13), the power allocation problem, aiming to maximize the sum rate, can be expressed as follows, when given the results of user grouping.

$$\max_{\mathbf{A}} \left\{ \sum_{l \in \mathcal{L}} U(\mathcal{S}_l) \mid \mathbf{M}^* \right\} , \tag{18}$$

$$\begin{aligned} s.t. \quad & (a) \sum_{k \in \mathcal{S}_l} \alpha_{k,l} = 1 \ , \forall l \in \mathcal{L} \\ & (b)\ 1 > \alpha_{k,l} > 0 \ , \forall k \in \mathcal{K}, \forall l \in \mathcal{L} \\ & (c)\ \frac{w_{k-1}}{w_k} \geq \frac{\alpha_{k,l}}{\alpha_{k-1,l-1}}, \forall k \in \mathcal{L}, \forall l \in \mathcal{L} \ . \end{aligned}$$

In above, condition (a) ensures that the sum of the power allocation within a coalition is one, and condition (b) specifies the range of the power coefficients. Further, constrain (c) is to avoid allocating the majority of the transmit power to the strongest user for the sake of the fairness. In the following, let us first introduce a pre-defined power allocation method, namely fractional power allocation. Then we propose the optimal algorithm to obtain the optimal power allocation.

B. Fractional Power allocation

In this section, we introduce a suboptimal transmission power control method, namely fractional power allocation (FPA), which is widely used [28]. In the FPA, the transmit power of CU_k in coalition $\mathcal{S}_l$ is allocated as follows:

$$\alpha_k = \frac{P_c H_{Ct,Cr_k}^{-\beta_{FPA}}}{\sum_k^K H_{Ct,Cr_k}^{-\beta_{FPA}}} \ . \tag{19}$$

where β_{FPA} is the decay factor, namely $0 \leq \beta_{FPA} \leq 1$. Additionally, the CUs within the same coalition are assumed to have the identical transmit power, when $\beta_{FPA} = 0$. As β_{FPA} increases, the CU with lower channel gain will be allocated more transmit power. Note that, the same value of β_{FPA} will be applied to the whole transmission period.

C. Optimal Power allocation

As described in Section II-B, the objective function of Eq. (18) is a monotonically and non-decreasing $\log(\cdot)$ function, which cannot affect the convexity of this problem. Apparently, Eq. (18) is not a convex problem. Then we obtain the following propositions.

Proposition 2: The optimization problem in (13) for power allocation is quasi-concave problem.

Proof:A maximization optimization problem is quasi-concave when the objective function is quasi-concave and the constraints are convex [29]. The conditions (a) and (b) in Problem (18) are convex, since both of them are linear.

It is observed that Problem (18) is NP-hard even though the existing of the convex constraints of (18)(a) and (18)(b) based on the theory in [30]. Hence, Problem (18) can be transformed into the sequence of linear programs and develop a customized low-complexity polynomial algorithm, in order to get its local optimal solution.

Let us first transform the origin problem of (18) into

$$\max_{\mathcal{A}} \left(\prod_{l \in \mathcal{L}} R_{l,w}^{CU} \right)^{\frac{w_l}{|\mathcal{S}_l|}} \tag{20}$$

where $R_{l,w}^{CU}$ has been defined in Eq. (12) and $|\mathcal{S}_l|$ is the number of players within the coalition $\mathcal{S}_l$. Based on the objective function of Eq. (20), we introduce two slack vectors $\mathbf{t} \in \mathbb{R}^{|\mathcal{S}_l|}$ and $\mathbf{b} \in \mathbb{R}_+^{|\mathcal{S}_l|-1}$ with the elements t_l and b_l, respectively. Then Eq. (20) can be rewritten as

$$\max_{\mathcal{A},b,t} \left(\prod_{l \in \mathcal{L}} t_l \right)^{\frac{1}{|\mathcal{S}_l|}} , \tag{21}$$

$$\begin{aligned} s.t. \quad & (a)\ |h_{Ct,Cr_k}|^2 P_c \alpha_{k,l} \geq (t_l - 1) b_l, \forall k, \forall l \in \mathcal{S}_l \\ & (b) |h_{Ct,Cr_k}|^2 P_c^2 \sum_{p=k+1}^{K} \alpha_{p,l} + P_p |h_{Pt,Cr_k}|^2 + \sigma^2 \leq b_l, \forall k, \forall l \in \mathcal{S}_l \\ & (c)\ 1 + \frac{|h_{Ct,Cr_K}|^2 P_c \alpha_{K,l}}{P_p |h_{Pt,Cr_k}|^2 + \sigma^2} \geq t_l \forall k, \forall l \in \mathcal{S}_l \\ & (d)\ \alpha_{1,l} \geq \cdots \geq \alpha_{k,l} \geq \cdots \geq \alpha_{K,l}, \\ & (e)\ 15(a)15(b) \end{aligned}$$

Additionally, the objective function of Eq. (21) is a geometric mean function, which is concave and increasing, respect to vector $\mathbf{t}$. Constraints (b) and (c) of Problem (21) are derived from Eq. (10) and Eq. (9). The original power allocation problem of (18) is equivalent to the transformation problem of (21). However, the objective function of Eq. (21) is still non-convex and intractable due to the bi-linear term in constraint (a). Therefore, we need to implement the further constraint (a) of (21) can be rewritten as $|h_{Ct,Cr_k}|^2 P_c \alpha_{l,k} \geq t_l b_l - b_l$. Hence, the transformation of this bi-linear term $t_l b_l$ can be computed as

$$t_l b_l = \frac{1}{4}[(t_l + b_l)^2 - (t_l - b_l)^2] \ . \tag{22}$$

It is observed that Eq. (22) is a non-convex function, and the term $(t_l + b_l)^2 - (t_l - b_l)^2$ of Eq. (22) is a difference between these two convex functions. Moreover, the second quadratic term on the right side of Eq. (22) can be approximated by its low bound, which is linear and is obtained by using Taylor series expansion, based on the convexity of itself. Then, we obtain the following first order Taylor approximation around the points $(t_l^{(n)}, b_l^{(n)})$ and is given by

$$\begin{aligned} f(t_l, b_l) &= (t_l - b_l)^2 \\ &\geq (t_l^{(n)} - b_l^{(n)})^2 + 2(t_l^{(n)} - b_l^{(n)})(t_l - t_l^{(n)} - b_l + b_l^{(n)}) \\ &\triangleq g(t_l, t_l^{(n)}, b_l, b_l^{(n)}), \end{aligned} \tag{23}$$

where $(t_l^{(n)}, b_l^{(n)})$ can be updated by $(t_l^{(n+1)}, b_l^{(n+1)})$). However, in every iteration the approximated inequality satisfies

This article has been accepted for publication in a future issue of this journal, but has not been fully edited. Content may change prior to final publication. Citation information: DOI 10.1109/ACCESS.2019.2910720, IEEE Access

the following conditions [31], [32], given by

$$f(t_l, b_l) \geq g(t_l, t_l^n bl, b_l^n) \ , \tag{24}$$

$$f(t_l^n, b_l^n) = g(t_l^n, t_l^n, b_l^n, b_l^n) \ , \tag{25}$$

$$\nabla f(t_l, bl)|_{(t_l^n, \beta_l^n)} = \nabla g(t_l, t_l^n, b_l, b_l^n)|_{(t_l^n, b_l^n)} \ . \tag{26}$$

Above, ∇f denotes the gradient of f. Further, the auxiliary variables (t_l, b_l) can be updated by $t_l^{(n+1)} = t_l^{(n)}$ and $b_l^{(n+1)} = b_l^{(n)}$, when condition (26) is satisfied in each iteration.

Hence, the problem of (21) can be converted to convex problem at the nth iteration by replacing $(t_l - b_l)^2$ with $g(t_l, t_l^{(n)}, b_l, b_l^{(n)})$, and it is given by

$$\max_{\mathbf{A},\mathbf{b},\mathbf{t}} \left(\prod_{l \in \mathcal{L}} t_l \right)^{\frac{1}{|\mathcal{S}_l|}} \ . \tag{27}$$

$$\begin{aligned} s.t. \ & (a) 4(|h_{Ct,Cr_k}|^2 P_c \alpha_{k,l} + b_k) + g(t_k, t_k^{(n)}, b_k, b_k^{(n)}) \\ & \geq (t_l + b_l)^2, s_i = 1, \ldots, K-1 \ , \\ & (b) 15(a), 15(b), 18(a), 18(b), 18(c) \ . \end{aligned}$$

Known from [33], Problem (27) is convex at the nth iteration round points $(t_l^{(n)}, b_l^{(n)})$. Therefore, we propose a successive iterative algorithm (SIA) to locally solve the approximation of Problem (27), which is related to the sequential convex approximation method [31]. As a result, the proposed optimal power allocation algorithm can be described in Algorithm 2.

Algorithm 2: Proposed successive iterative algorithm (SIA) for solving the problem of Eq. (27)

1 *Initial state*: Set $(t_l^{(n)}, b_l^{(n)})$ of Problem (27) while $n = 0$.
2 *Repeat*
1) Solve Problem (27) with $(t_l^{(n)}, b_l^{(n)})$ to get the optimal values (t_l^*, b_l^*).
2) Set $n \to n+1$, update $(t_l^{(n+1)}, b_l^{(n+1)}) = (b_l^*, t_l^*)$.
until Converge.
Output the optimal solution of Problem (27).

D. Convergence Analysis

In this section, we analyze the convergence of the proposed SIA algorithm as shown in Algorithm 2. Let us define the feasible set as $\mathcal{Z}^{(n)}$ and the sequence of variables set as $\mathcal{B}^{(n)} = [t_l^{(n)}, b_l^{(n)}]$, for all s_i in the nth iteration of the problem in Eq. (27). Furthermore, we assume that feasible set of the problem in Eq. (21) as $\mathcal{Z}$. Then, we readily obtain the Proposition 3.

Proposition 3: The sequence of variables $\mathcal{B}^{(n)}$ belongs to $\mathcal{Z}$. By defining the objective value of Eq. (27) as $\mathcal{F}^{(n)}$, we have $\mathcal{F}^{(n+1)} \geq \mathcal{F}^{(n)}$, and the algorithm converges.

Proof: In order to prove $\mathcal{B}^{(n)}$ belongs to $\mathcal{Z}$, we only need to prove $\mathcal{Z}^{(n)}$ is included in $\mathcal{Z}$. Since $\mathcal{B}^{(n)}$ is the optimal solution for Problem (27), the sequence of variables $\mathcal{B}^{(n)}$ belongs to $\mathcal{Z}^{(n)}$, such that $\mathcal{B}^{(n)} \in \mathcal{Z}^{(n)}$. We assume that the variables $t_l^{(n)^*}$ and $b_l^{(n)^*}$ are the optimal solutions for Problem (27) at the nth iteration. Then $t_l^{(n)^*}$ and $b_l^{(n)^*}$ belong to the feasible set $\mathcal{Z}^{(n)}$ and they satisfy the all the constraints of Problem (27). We can clearly prove that $t_l^{(n)^*}$ and $b_l^{(n)^*}$ also satisfy all constraints in Problem (21). That is because we employ the convex approximation $g(t_l, t_l^{(n)}, b_l, b_l^{(n)})$ for $(t_l - b_l)^2$ and the conditions in Eq.(26). Hence, $\mathcal{Z}^{(n)}$ is included in $\mathcal{Z}$ and the sequence of variables $\mathcal{B}^{(n)}$ belongs to $\mathcal{Z}$. Since the point $(t_l^{(n+1)}, b_l^{(n+1)})$ at the $n+1$th iteration is updated by the sequence of variables $\mathcal{B}^{(n)}$ at the nth iteration, the point $(t_l^{(n+1)}, b_l^{(n+1)})$ belongs to the feasible set of Problem (27) at the $n+1$th iteration. Furthermore, Problem (27) have been solved by using the proposed SIA of Algorithm 2, which generates a non-decreasing sequence of objective values, i.e. $\mathcal{F}^{(n+1)} \geq \mathcal{F}^{(n)}$. According to the proposition 2, the proposed iterative algorithm converges to a finite value. However, we cannot prove the algorithm converges to the global optimum solution, due to the original problem of (21) is non-convex.

In the following proposition, we will prove that our proposed algorithm satisfies the Karush-Kuhn-Tucker (KKT) conditions.

Proposition 4: Algorithm 2 converges to the KKT point of Problem (21) when it achieves the pre-defined accuracy.
Proof: Please, refer to Appendix I.

V. Simulation Results and Discussion

In this section, we provide the rate performance of the underlay CR-NOMA network considered. In particular, the performance analysis is carried out for the proposed DSCF algorithm and the optimal power allocation algorithm by comparing with the other algorithms. The main assumptions in our simulations are summarized in Table II.

K: Total number of CU	20
Number of realizations	10^5
P_P: Transmit power of PU	15dB
P_S: Transmit power of CU	10dB
η: Scale factor	0.8
a: Pathloss exponent	3

TABLE II
The parameters of our CR-NOMA system.

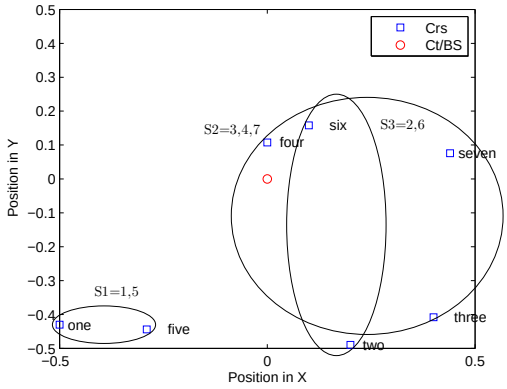

Fig. 2. Final coalition structure from proposed algorithm in underlay CR-NOMA scheme when $K = 7$.

This article has been accepted for publication in a future issue of this journal, but has not been fully edited. Content may change prior to final publication. Citation information: DOI 10.1109/ACCESS.2019.2910720, IEEE Access

In Fig. 2, we show a snapshot of the network structure resulting from the proposed DSCF algorithm for a scenario that $K = 7$ random Crs are deployed in the square area. Seen from the simulations results of Fig. 2, CU_1, CU_2 and CU_7 are setting as the three fixed coalitions, since their corresponding channel gains are below the threshold, as described in Section III-B. Further, we find that CU_4 has the best channel condition among the seven CUs, thereby giving it the highest priority to select its best suitable partition. However, this active CU_4 merges with CU_7 due to the fact that, $CU_1 \triangleright CU_2 \triangleright CU_7$, and the corresponding utilities of CU_4 in these three partitions are $\mathcal{U}_4 = 3.5407$, $\mathcal{U}_4 = 5.0819$, $\mathcal{U}_4 = 5.3292$. Following the above principles, we obtain the three stable coalitions which are $\mathcal{S}_1 = \{1, 5\}$, $\mathcal{S}_2 = \{2, 6\}$ and $\mathcal{S}_3 = \{7, 4, 3\}$. Additionally, their relative utilities for the partitions are given in Table III. In Table III, it proves that our DSCF algorithm converges to a stable coalition structure, since all the players satisfy with their current coalitions and no one has an incentive to leave its current coalition.

Fixed coalition head	Cr_4	Cr_6	Cr_5	Cr_3
Cr_1	3.5407	2.9208	**2.8314**	0.7539
Cr_2	5.0819	**4.4121**	0.6430	0.8270
Cr_7	**5.3292**	0.8917	0.9118	**0.9522**

TABLE III
THE INDIVIDUAL UTILITY OF ACTIVE USERS AFTER JOIN INTO THE FIXED COALITIONS.

In Section IV, we compare the proposed optimal power allocation with the FPA algorithm. In particular, Fig. 3 illustrates the sum rate of all the CUs in our CR-NOMA network versus the total number of CUs, where the FPA scheme is evaluated with different decay factor values. Seen from the figure, with the increasing value of β_{FPA}, the sum rate of all the CUs decreases, which is due to, the most transmit power is allocated to the user with poor channel gain, based on (19). Hence, the total CU's utility increases when using smaller value of β_{FPA}. Without loss of generality, in the following simulations, $\beta_{FPA} = 0.8$ is employed for the FPA scheme.

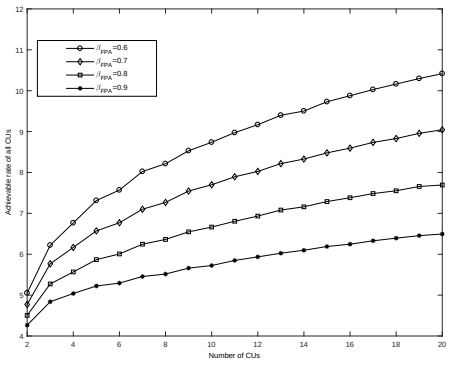

Fig. 3. The Number of CUs versus the total utility of all the when considering the fractional power allocation with the different decay factor β_{FPA}.

Fig. 4 shows the number of CUs versus the total system rate of both the PU and the selected CU group, by using two methods of power allocation as described in Section IV-A, where the transmit power of CUs is $Ps = 10dB$ and the transmit power of PU is $Pp = 15dB$. Note that, in Fig. 4, the curves labelled by "NOMA-SIR" represents that the optimal power allocation scheme is used, as shown in Table 2. In Fig. 4, the performance of employing the optimal power allocation scheme is much better than that of the fractional power allocation scheme. Specifically, when $K = 16$, the SIA aided underlay CR-NOMA system achieves the sum rate which can be almost six times higher than that for the FPA aided system. Furthermore, as seen from Fig. 4 that our CR-NOMA system always achieve a higher sum-rate than that of the Orthogonal Multiple Access (OMA) system, regardless of the user grouping and power allocation approaches used. Furthermore, we have consider two benchmarks, namely centralized algorithm (CA) as well as the Random algorithm (RA), which are respectively taken as the upper bound and lower bound of the considered CR-NOMA system. In the considered CA, we select the best CU group, which has the maximum sum-rate according to our intended objective functions as shown in Eq. (16), from all possible CU groups with the aid of exhaustive search approach. Then, in the context of the CA scheme, the SIA power allocation is applied to the selected CU group. Nevertheless, the CA requires extremely high number of operations/complexity, which becomes impractical when the number of CUs is large. Seen from Fig. 4, the performance of our considered CR-NOMA system by employing the DSCF algorithm and the optimal power allocation, is close to the centralized solution. Moreover, the performance of the RA, in which the CUs are randomly selected, is much worsen than that of the DSCF algorithm, albeit better than that of the OMA scheme.

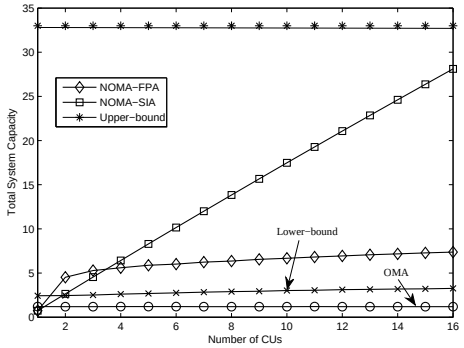

Fig. 4. The Number of CUs versus the total system rate, while $P_S = 10$dB, $P_p = 15$dB and $\beta_{FPA} = 0.8$.

In Fig. 5, it evaluates the size of the chosen CU group in terms of the PU's demand η while considering the different number of CUs, K. Without loss of generality, let us set the transmit power of the PU as $P_p = 15dB$. It is observed that the average size of the chosen coalition decreases as the PU's demand η increases. That is because the CUs are less likely to satisfy the PU's demand when the PU increases its demand, which leads to the decreasing of the chosen coalition's size. Additionally, the average size of the chosen coalition increases as more CUs decide to join in the CR network. Thus, these joined CUs provide a variety of partition patterns. The CUs are more likely to satisfy the PU's demand and get the opportunity

This article has been accepted for publication in a future issue of this journal, but has not been fully edited. Content may change prior to final publication. Citation information: DOI 10.1109/ACCESS.2019.2910720, IEEE Access

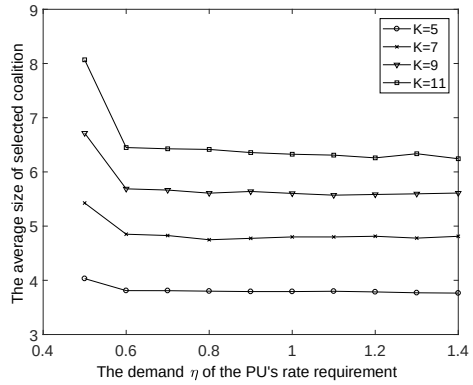

Fig. 5. Size of coalition with different values of the PU's demand.

to access the spectrum. Therefore, the chosen coalition's size increases with the increasing number of the CUs. Additionally, the average size of chosen coalition converges to a certain value in Fig. 5, that is because we normally chosen one coalition who will provide the highest sum rate at the end of the game.

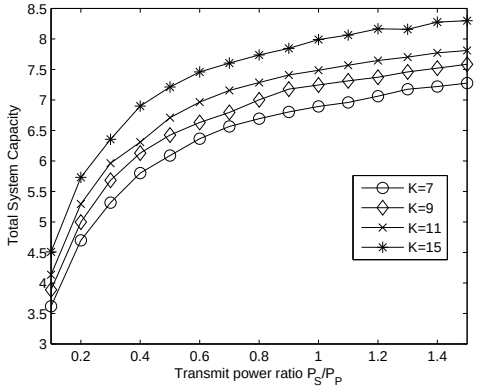

Fig. 6. Total system rate versus the transmit power ratio between the transmit power of the CUs, P_S, and the transmit power of the PU,P_P, while $\beta_{FPA} = 0.8$.

In Fig. 6, it investigates the total system rate of our considered CR-NOMA system when considering different values of the CU's maximum transmit power P_s. For this scenario, let us set the PU's demand as $\eta = 0.7$. We can see that the sum rate of the CUs increases together with CUs' transmit power P_S in the beginning. When the transmit power P_P is larger than the P_S, the CUs' utility becomes smaller. This observation can be interpreted as the followings. When P_S is approximately zero, the PU's demand cannot be satisfied. Therefore, the CUs cannot access the spectrum. Thus, the CUs' sum rate is positively correlated with their transmit power P_S . Additionally, in Fig. 6, we assume that the transmit power of the PU is at a certain value. Furthermore, Fig. 7 demonstrates the fairness of the system with the different values of decay factor β_{FPA}. We have considered the Jain's fairness $(\sum_k^K R_k)^2/N\sum_k^K R_k^2$ [34]. By observing from Fig. 7, the fairness is decreasing with the increasing number of the CUs. Moreover, the fairness is increasing with the increasing value of the decay factor.

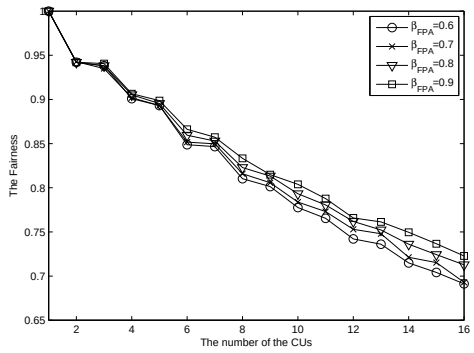

Fig. 7. Fairness versus the number of the CUs.

VI. Practical Code and Modulation Design

In this section we investigate the practical design of the CR-NOMA system advocated using ATTCM. Employing TTCM has the advantage that the system's effective throughput can be increased upon increasing the code rate, when the channel-quality improves. Additionally, the Bit error ratio (BER) performance of the system may be improved when TTCM is used [35]. The TTCM encoder comprises two identical parallel-concatenated TCM encoders [36] linked by a symbol interleaver. The first TCM encoder directly processes the original input bit sequence, while the second TCM encoder manipulates the interleaved version of the input bit sequence. Then the bit-to-symbol mapper maps the input bits to complex-valued ATTCM symbols using the Set Partition based labelling method [35]. The structure of the TTCM decoder is similar to that of binary turbo codes, but each decoder alternately processes its corresponding encoder's channel-impaired output symbol, and then the other encoder's channel-impaired output symbol [35, p.764]. More details on the ATTCM principles can be found in [35].

We have employed a ATTCM scheme for the considered CR-underlay system, where the information Bit-per-Symbol (iBPS) is selected from the set iBPS$=\{0, 1, 2, 3, 5\}$ Bit-per-Symbol (BPS) corresponding to the case of no transmission, QPSK, 8PSK, 16QAM and 64QAM modulations, respectively. Moreover, the ATTCM mode switching thresholds Υ =$[\gamma_0, \gamma_1, \gamma_2, \gamma_3]$ were determined based on the BER performance curves of each of the four TTCM schemes in a Rayleigh fading channel, which is shown in Fig. 8. Specifically, the ATTCM mode switching operation and the throughput of the modes are specified by the following algorithm:

$$\text{MODE} = \begin{cases} \gamma_3 \le \gamma_R, & \text{TTCM-64QAM, iBPS=5 BPS;} \\ \gamma_2 \le \gamma_R < \gamma_3, & \text{TTCM-16QAM, iBPS=3 BPS;} \\ \gamma_1 \le \gamma_R < \gamma_2, & \text{TTCM-8PSK, iBPS=2 BPS;} \\ \gamma_0 \le \gamma_R < \gamma_1, & \text{TTCM-4PSK, iBPS=1 BPS;} \\ \gamma_R < \gamma_0, & \text{No transmission, iBPS=0 BPS.} \end{cases}$$

We use the notation γ_R^{CU} represents the instantaneous received SNR of the link between the CUs' BS and the CU$_k$. The received SNR of CU$_k$ within a selected coalition $\mathcal{S}_i$ is given

This article has been accepted for publication in a future issue of this journal, but has not been fully edited. Content may change prior to final publication. Citation information: DOI 10.1109/ACCESS.2019.2910720, IEEE Access

by [13]

$$\gamma_{R,k}^{CU}(\mathcal{S}_i) = \frac{\alpha_k P_S |h_{ct,cr_k}|^2}{\sum_p^{|\mathcal{S}_i|}(\alpha_p) P_S + N_0}. \quad (28)$$

The received SNR of the last CU_P within $\mathcal{S}_i$ can be expressed as:

$$\gamma_{R,P}^{CU}(\mathcal{S}_i) = \frac{\alpha_P P_S |h_{ct,cr_P}|^2}{N_0}, \quad (29)$$

where $P \leq K$ and the term α_k is the power allocation coefficient of CU_k, P_S is the transmit power emit from the CUs' BS is detailed in Section II. The quasi-static Rayleigh fading channels between the CU's BS and CU_k is denoted as h_{ct,cr_k}. Therefore, the channel gains of each CU is independent of each other.

Each of the communication links in our considered CR-underlay system will be assisted by the ATTCM scheme. We chose the switching thresholds to ensure that the target BER is lower than 10^{-5}, which is given by Υ_{ATTCM}=[4.8, 12, 16, 24] dB as seen in Fig. 8.

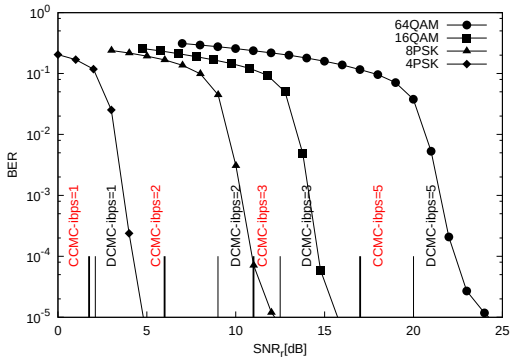

Fig. 8. BER versus SNR_r of TTCM using a frame length of 120,000 symbols, when communicating over Rayleigh fading channels. Four TTCM iterations were invoked.

The reason why we have chosen the target BER to be lower than 10^{-5} is because the error floor emerging at BER$< 10^{-5}$ can be removed by using a long outer code, such as a Reed Solomon (RS) code, albeit no RS code was used here. For quasi-static fading channels, the achievable rates over different links become random and vary as the channel changes. The relatively performances of our ATTCM aided underlay CR network will be discussed in following Section.

In Fig. 9, we investigate the performance of the ATTCM aided CR-NOMA systems by employing the DSCF as well as the appropriate fractional power allocation among the selected coalition groups. By observing Fig. 9, the system capacity of the CUs decrease while increasing the transmit power P_s. That is because the CUs' sum rate is positively correlated with their transmit power P_S. These two factors contribute to CUs' low sum rate when their transmit power P_S is big. When this transmit power P_S increases, CUs' sum rate can either increase or decrease. On one hand, CUs' increasing transmit power leads to the increase of CUs' sum rate. On the other hand, the interference generated by CUs increases with CUs' increasing transmit power P_S. The strong interference may be harmful to the PU's achievable rate and leads to the absence of

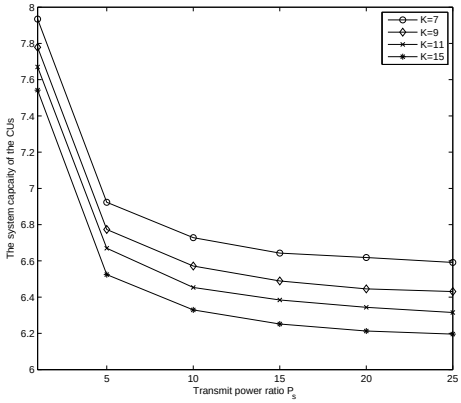

Fig. 9. Performance of total sum rate of our considered CR-NOMA with the different transmit power of the CUs P_S, while the transmit power of PU is $P_p = 10$ and the assumed the decay factor value of power allocation is $\beta_{FPA} = 0.8$.

CUs. Therefore, CUs' sum rate decreases when their transmit power P_S is strong enough.

VII. Conclusions

In this paper, we have studied the resource allocation in the underlay CR network in which NOMA scheme is employed. In particular, the joint user grouping and power allocation problem has been investigated. With the aid of the NTU coalition formation game model, we have proposed the DSCF algorithm to solve the decoupled CU grouping problem. Then, the optimal power allocation algorithm has been developed by solving the non-convex optimization problem, which can be converted to the convex ones with the help of first order Taylor series approximation and the other related manipulations. We have shown that the proposed DSCF algorithm can converge to a Nash-stable and has a low complexity compared to the benchmark considered, namely CA algorithm, as well as the other existing algorithms. Our numerical analysis has revealed that the final stable partitions by employing the SIA algorithm, i.e. the optimal power allocation, can significantly outperform the existing FPA power allocation. Furthermore, our simulation results have shown that, the considered underlay CR-NOMA scheme can achieve obvious performance advantage over the traditional CR-OMA scheme. In the end, we have investigated a practical ATTCM scheme can be applied to the CR-NOMA system, and the achievable throughput can be further enhanced according to our simulation results.

Appendix I

Let us define an accumulation point $\mathcal{B}^*$ of the sequence of variables $\mathcal{B}^{(n)}$ at convergence. We first need to simplify the constraints in the original problem Eq. (21) and the approximation problem Eq. (27). Since the only difference in the constraints of both problems is the first constraint, we set the remain constraints as a function $G_k(\mathcal{B})$. The approximation problem (27) satisfies the Slater's conditions since it is strictly convex program [33]. Then, the KKT conditions of Eq. (27) at the accumulation point $\mathcal{B}^*$ can be expressed as following

with the optimal dual variables λ_k^*, μ_k^*

$$\nabla f_0(t_k^*) - \sum_{k=1}^{K-1} \lambda_k^* \big(g(t_k^*, t_k^{(*)}, \beta_k^*, \beta_k^{(*)}) - A_k^*\big) + \sum_{k=1}^{K} \mu_k^* G_k(\mathcal{B}^*) = 0 \quad (30)$$

$$\lambda_k^* \big(g(t_k^*, t_k^{(*)}, \beta_k^*, \beta_k^{(*)}) - A_k^*\big) = 0 \quad (31)$$

$$\mu_k^* G_k(\mathcal{B}^*) = 0. \quad (32)$$

where $A_k^* = (t_k^* + \beta_k^*)^2 - 4(|h_{Ct,Cr_k}|^2 P_c \alpha_k^* + \beta_k^*)$. According to the equality condition Eq. (23), we know $(t_k^* - \beta_k^*)^2 = f(t_k^*, \beta_k^*) = g(t_k^*, t_k^{(*)}, \beta_k^*, \beta_k^{(*)})$. Then replacing $g(t_k^*, t_k^{(*)}, \beta_k^*, \beta_k^{(*)})$ by $(t_k^* - \beta_k^*)^2$, the above KKT conditions can be reformulated as

$$\nabla f_0(t_k^*) - \sum_{k=1}^{K-1} \lambda_k^* \big((t_k^* - \beta_k^*)^2 - A_k^*\big) + \sum_{k=1}^{K} \mu_k^* G_k(\mathcal{B}^*) = 0 \quad (33)$$

$$\lambda_k^* \big((t_k^* - \beta_k^*)^2 - A_k^*\big) = 0 \quad (34)$$

$$\mu_k^* G_k(\mathcal{B}^*) = 0. \quad (35)$$

It is clearly shown that the reformulated KKT conditions above are also the KKT conditions of the original problem of Eq. (21). Therefore, the convergent point $\mathcal{B}^*$ generated by the proposed algorithm is a KKT point of Eq. (21).

REFERENCES

[1] S. Haykin, "Cognitive radio: brain-empowered wireless communications," *IEEE Journal on Selected Areas in Communications*, vol. 23, pp. 201 – 220, Feb. 2005.

[2] A. Goldsmith, S. Jafar, I. Maric, and S. Srinivasa, "Breaking spectrum gridlock with cognitive radios: An information theoretic perspective," *Proceedings of the IEEE*, pp. 894 –914, May 2009.

[3] W. Liang, S. X. Ng, and L. Hanzo, "Cooperative overlay spectrum access in cognitive radio networks," *IEEE Communications Surveys Tutorials*, vol. 19, pp. 1924–1944, thirdquarter 2017.

[4] Y. Saito, A. Benjebbour, Y. Kishiyama, and T. Nakamura, "System-level performance evaluation of downlink non-orthogonal multiple access (NOMA)," in *IEEE 24th International Symposium on Personal Indoor and Mobile Radio Communications (PIMRC)*, pp. 611–615, Sept 2013.

[5] Y. Saito, Y. Kishiyama, A. Benjebbour, T. Nakamura, A. Li, and K. Higuchi, "Non-Orthogonal Multiple Access (NOMA) for Cellular Future Radio Access," in *IEEE 77th Vehicular Technology Conference (VTC Spring)*, pp. 1–5, June 2013.

[6] S. L. Shieh and Y. C. Huang, "A Simple Scheme for Realizing the Promised Gains of Downlink Nonorthogonal Multiple Access," *IEEE Transactions on Communications*, vol. 64, pp. 1624–1635, April 2016.

[7] J. Choi, "Minimum Power Multicast Beamforming With Superposition Coding for Multiresolution Broadcast and Application to NOMA Systems," *IEEE Transactions on Communications*, vol. 63, pp. 791–800, March 2015.

[8] Z. Ding, M. Peng, and H. Poor, "Cooperative Non-Orthogonal Multiple Access in 5G Systems," *IEEE Communications Letters*, vol. 19, pp. 1462–1465, Aug 2015.

[9] J. B. Kim and I. H. Lee, "Non-Orthogonal Multiple Access in Coordinated Direct and Relay Transmission," *IEEE Communications Letters*, vol. 19, pp. 2037–2040, Nov 2015.

[10] Z. Ding, F. Adachi, and H. Poor, "The Application of MIMO to Non-Orthogonal Multiple Access," *IEEE Transactions on Wireless Communications*, vol. 15, pp. 537–552, Jan 2016.

[11] H. Marshoud, V. M. Kapinas, G. K. Karagiannidis, and S. Muhaidat, "Non-orthogonal multiple access for visible light communications," *IEEE Photonics Technology Letters*, vol. 28, pp. 51–54, Jan 2016.

[12] Y. Liu, Z. Ding, M. Elkashlan, and H. V. Poor, "Cooperative non-orthogonal multiple access with simultaneous wireless information and power transfer," *IEEE Journal on Selected Areas in Communications*, vol. 34, pp. 938–953, April 2016.

[13] W. Liang, Z. Ding, Y. Li, and L. Song, "User pairing for downlink non-orthogonal multiple access networks using matching algorithm," *IEEE Transactions on Communications*, vol. 65, pp. 5319–5332, Dec 2017.

[14] Y. Zhang, H. M. Wang, Q. Yang, and Z. Ding, "Secrecy sum rate maximization in non-orthogonal multiple access," *IEEE Communications Letters*, vol. 20, pp. 930–933, May 2016.

[15] Y. Liu, Z. Ding, M. Elkashlan, and J. Yuan, "Nonorthogonal multiple access in large-scale underlay cognitive radio networks," *IEEE Transactions on Vehicular Technology*, vol. 65, pp. 10152–10157, Dec 2016.

[16] L. Lv, Q. Ni, Z. Ding, and J. Chen, "Application of non-orthogonal multiple access in cooperative spectrum-sharing networks over nakagami- m fading channels," *IEEE Transactions on Vehicular Technology*, vol. 66, pp. 5506–5511, June 2017.

[17] L. Lv, J. Chen, Q. Ni, Z. Ding, and H. Jiang, "Cognitive non-orthogonal multiple access with cooperative relaying: A new wireless frontier for 5g spectrum sharing," *IEEE Communications Magazine*, vol. 56, pp. 188–195, APRIL 2018.

[18] W. Saad, Z. Han, M. Debbah, and A. Hjorungnes, "A distributed merge and split algorithm for fair cooperation in wireless networks," in *ICC Workshops - 2008 IEEE International Conference on Communications Workshops*, pp. 311–315, May 2008.

[19] H. Zhang, T. Wang, L. Song, and Z. Han, "Interference Improves PHY Security for Cognitive Radio Networks," *IEEE Transactions on Information Forensics and Security*, vol. 11, pp. 609–620, March 2016.

[20] Z. Dai and V. W. S. Wong, "Traffic demand-based cooperation strategy in cognitive radio networks," in *2014 IEEE Wireless Communications and Networking Conference (WCNC)*, pp. 1832–1837, April 2014.

[21] W. Saad, Z. Han, M. Debbah, A. Hjorungnes, and T. Basar, "Coalitional games for distributed collaborative spectrum sensing in cognitive radio networks," in *IEEE INFOCOM 2009*, pp. 2114–2122, April 2009.

[22] R. Zhang, L. Song, Z. Han, X. Cheng, and B. Jiao, "Distributed resource allocation for device-to-device communications underlaying cellular networks," in *2013 IEEE International Conference on Communications (ICC)*, pp. 1889–1893, June 2013.

[23] Y. Chen, B. Ai, Y. Niu, K. Guan, and Z. Han, "Resource allocation for device-to-device communications underlaying heterogeneous cellular networks using coalitional games," *IEEE Transactions on Wireless Communications*, vol. 17, pp. 4163–4176, June 2018.

[24] W. Liang, S. Ng, J. Feng, and L. Hanzo, "Pragmatic distributed algorithm for spectral access in cooperative cognitive radio networks," *IEEE Transactions on Communications*, vol. 62, pp. 1188–1200, April 2014.

[25] J. Zou, H. Xiong, D. Wang, and C. W. Chen, "Optimal power allocation for hybrid overlay/underlay spectrum sharing in multiband cognitive radio networks," *IEEE Transactions on Vehicular Technology*, vol. 62, pp. 1827–1837, May 2013.

[26] S. Mathur, L. Sankar, and N. B. Mandayam, "Coalitions in cooperative wireless networks," *IEEE Journal on Selected Areas in Communica*, vol. 26, no. 7, pp. 1104–1115, 2008.

[27] J. Jalden and B. Ottersten, "On the complexity of sphere decoding in digital communications," *IEEE Transactions on Signal Processing*, vol. 53, pp. 1474–1484, April 2005.

[28] A. Benjebbovu, A. Li, Y. Saito, Y. Kishiyama, A. Harada, and T. Nakamura, "System-level performance of downlink NOMA for future LTE enhancements," in *2013 IEEE Globecom Workshops (GC Wkshps)*, pp. 66–70, Dec 2013.

[29] S. Boyd and L. Vandenberghe, *Convec Optimization*. Cambridge University Press, 2004.

[30] Z.-Q. Luo and S. Zhang, "Dynamic spectrum management: Complexity and duality," *IEEE J. Sel. Topics Signal Process*, vol. 2, pp. 57–73, Jan 2008.

[31] A. B. T. A. Beck and L. Tetruashvili, "A sequential parametric convex approximation method with applications to nonconvex truss topology design problems," *J. Global Opt.*, vol. 47, no. 1, pp. 29–51, 2010.

[32] M. F. Hanif, Z. Ding, T. Ratnarajah, and G. K. Karagiannidis, "A minorization-maximization method for optimizing sum rate in nonorthogonal multiple access systems," *IEEE Trans. Signal Process*, vol. 64, pp. 76–88, Jan 2016.

[33] S. Boyd and L. Vandenberghe, "Covex optimization," *Cambridge Univ. Press*, 2004.

[34] R. Jain, D.-M. Chiu, and W. R. Hawe, "A quantitative measure of fairness and discrimination for resource allocation in shared computer system," *Eastern Research Laboratory, Digital Equipment Corporation Hudson*, vol. 38, 1984.

[35] L. Hanzo, S. X. Ng, T. Keller, and W. Webb, *Quadrature Amplitude Modulation:From Basics to Adaptive Trellis-Coded, Turbo-Equalised and Space-Time Coded OFDM, CDMA and MC-CDMA Systems*. Wiley-IEEE Press, 2004.

[36] G. Ungerböck, "Channel coding with multilevel/phase signals," *IEEE Transactions on Information Theory*, vol. 28, pp. 55–67, January 1982.